

Published in final edited form as:

J Occup Environ Hyg. 2012 ; 9(3): 129–139. doi:10.1080/15459624.2011.652061.

A Novel Device for Measuring Respirable Dustiness Using Low Mass Powder Samples

Patrick T. O'Shaughnessy, Mitchell Kang, and Daniel Ellickson

Occupational and Environmental Health, College of Public Health, 100 Oakdale Campus, IREH, The University of Iowa, Iowa City, Iowa

Abstract

Respirable dustiness represents the tendency of a powder to generate respirable airborne dust during handling and therefore indicates the propensity for a powder to become an inhalation hazard. The dustiness of fourteen powders, including ten different nanopowders, was evaluated with the use of a novel low mass dustiness tester (LMDT) designed to minimize the use of the test powder. The aerosol created from 15-mg powder samples falling down a tube were measured with an aerodynamic particle sizer (APS). Particle counts integrated throughout the pulse of aerosol created by the falling powder were used to calculate a respirable dustiness mass fraction (D, mg/kg). An amorphous silicon dioxide nanopowder produced a respirable D of 121.4 mg/kg which was significantly higher than all other powders ($p < 0.001$). Many nanopowders produced D values of that were not significantly different from large-particle powders such as Arizona Road Dust and Bentonite clay. In general, fibrous nanopowders and powders with primary particles > 100 nm are not as dusty as those containing granular, nano-sized primary particles. The method used here, incorporating an APS, represents a deviation from a standard method but resulted in dustiness values comparable to other standard methods.

Keywords

nanoparticle; dustiness; risk assessment

INTRODUCTION

Given the rise in products developed with the use of nanotechnology, it is unclear if this technology will lead to new or unidentified risks to human health.^(1,2) In particular, little is known about how to safely handle nanoparticles, or what, if any, immediate risks may arise from inhaling nanoparticles in an occupational environment.⁽³⁾ Furthermore, there is some uncertainty as to the best exposure metric, as well as a lack of proper equipment to measure them at their source of production.⁽²⁾ To address these limitations, more strategic and risk-related research is necessary to ensure that people working in nanotechnology industries are protected from adverse health effects caused by aerosolized nanopowders.

Excessive airborne dust levels in occupational settings are undesirable because: they can cause adverse health effects, can be costly to control or costly in terms of lost product, and can contaminate machinery and products.⁽⁴⁾ Thus, it is advantageous to have detailed information about the propensity of nanoparticles to become airborne if emitted as a fugitive dust – that is, their “dustiness” – to fully characterize the risks involved with their production. Dustiness is generally considered to be the propensity of a powder to produce

Address correspondence to: Patrick O'Shaughnessy, Occupational and Environmental Health, College of Public Health, 100 Oakdale Campus, 137 IREH, Iowa City, IA 52242; patrick-oshaughnessy@uiowa.edu.

airborne dust as a result of handling the powder, which includes storing, filling, conveying and mixing.^(2, 5–8) Therefore, a potential hazard of nanotechnology is related to the dustiness of the nanoparticle bulk powder when handled during the production of nanomaterials.⁽⁵⁾

As provided in previous papers addressing this subject,^(8–10) the identification of a powder's dustiness may aid in the predication of occupational dust exposure and is therefore a meaningful health-risk attribute when assessing their overall risk to workers. For example, Shulte et al. advocate for the use of dustiness as a risk parameter when utilizing a control banding approach to manage exposures to engineered nanoparticles.⁽¹⁰⁾ Likewise, Schneider et al. suggest that dustiness tests can be translated to estimates of workplace exposures as part of a comprehensive conceptual model of nanoparticle exposures used as the basis of a nanoparticle risk assessment strategy.⁽¹¹⁾ However, a direct link between powder dustiness and worker exposure has been difficult to verify. As summarized by Liden,⁽⁸⁾ studies conducted to relate dustiness to worker exposure^(6,9,12,13) have shown a positive correlation between the two, but other factors such as control technologies and powder handling may often contribute more to overall exposure than the dustiness of the powder. Therefore Liden suggests that dustiness should be viewed as a risk factor contributing to the “source strength” of potential aerosol generation rather than as a surrogate for occupational exposure.

A number of factors will affect the dustiness of a powder. Pujara and Kildig discuss these properties and review the available literature on this topic.⁽¹⁴⁾ They identify powder mass, bulk density, and moisture content, as well as particle shape, size and cohesion as the most important factors determining the dustiness of a powder, with size being the most influential. Boundy et al. add factors such as powder surface chemistry and prior handling, such as whether the powder was previously compressed or dried, as also affecting powder dustiness.⁽¹⁵⁾

Standard methods for determining the dustiness of powders have been developed in Europe, but not in the United States. For example, the German standard, DIN 55992-2⁽¹⁶⁾, describes the single-drop method to determine the dustiness index for pigments and fillers for quality control purposes. Whereas, the European standard, EN 15051⁽¹⁷⁾, utilizes a rotating drum or a continuous drop device to create a dust cloud. These methods are well described by Hamelmann and Schmidt^(5,7) and are briefly reviewed here.

The single-drop dustiness device is comprised of a vertical tube that generates dust by placing a sample on a shutter atop the tube then opening the shutter allowing the sample to drop through the tube into a chamber at the bottom. The resulting cloud of dust is measured over time with an aerosol photometer viewing the particle cloud in the chamber. Following DIN 55992-2, dustiness is indicated by computing the ratio of the integrated concentration from 16 – 30 s to the integrated concentration from 1 – 30 s. No explanation for the significance of the 16-second start value in the numerator integral is provided. However, Bach and Schmidt used a commercial version of this apparatus, the Palas Dustview (Palas GmbH, Karlsruhe, Germany), and chose the concentrations at 0.5 s and 30 s as representative of the inhalable and respirable fraction of dust, respectively.⁽¹⁸⁾ The device, therefore, provides a dustiness “characteristic” of the test powder since the concentration value obtained is not related to the mass of powder applied to the device.

The rotating drum apparatus, as the name suggests, supplies mechanical energy to a bulk sample with the use of a rotating drum. The Heubach dust meter, originally developed to determine the dustiness of pigments, is an example of a rotating drum dustiness tester that has been evaluated for use as a dustiness tester for powders of occupational health significance.^(18–20) With this device, a steady stream of air is supplied through the drum and

exiting particles are collected on a filter or measured with a direct-reading instrument. Unlike the single-drop device, the rotating drum provides a dustiness “mass fraction” by calculating the ratio of the mass collected on the filter after 1 min to the mass of powder supplied to the device.⁽¹⁸⁾ If the aerosol sampling device has a size-selective inlet, then the dustiness mass fraction can be segregated between respirable and inhalable dust. This technique is employed by the rotating drum device described in EN 15051. However, use of that device requires between 300–600 g of bulk powder. Schneider and Jensen augmented the method so that only 8 g was needed by employing an Aerodynamic Particle Sizer (APS, TSI Inc., Shoreview, MN).⁽²¹⁾

EN 15051 also describes a continuous drop dustiness tester.⁽¹⁷⁾ Dust is continuously augured into a 1.1 m by 150 mm tube which meets an upward flow of air pulled at a rate 53 L min⁻¹. Sample inlets to measure the inhalable and respirable size fractions of dust generated are located 0.8 m up from the bottom of the tube. Only one study could be found that used this method⁽²²⁾ where a weak correlation was found between the dustiness values obtained with this method and that of the rotating drum.

This study was motivated by the need for a nanopowder dustiness measurement technique that utilized milligram quantities of test powder and could size-segregate particles in the dust cloud. The first criterion is related to the large expense of some nanopowders such as purified single-walled carbon nanotubes (~\$250.00 US/gm). Of the available standard methods, only the single-drop device could achieve that goal. However, following DIN 55992-2 does not allow for either a verifiable aerosol size-segregation process or the calculation of a dustiness mass fraction useful for risk assessment efforts. Therefore, the objective of this study was to develop a single-drop tester that could meet those criteria.

METHODS

Dustiness-Test Apparatus

The low mass dustiness tester (LMDT) was developed similar to that recommended in DIN 55992-2 with some modifications. A ball valve was attached to the top end of an inverted 9.53-mm (3/8”) I.D. by 0.61 m (24”) long chrome-plated brass pipe (Figure 1). A 3.5 cm I.D. by 7.6 cm long polyvinyl chloride (PVC) tube with 1.25 cm wall thickness was bored and threaded perpendicular to its center to receive the bottom of the drop pipe. A similar hole on the bottom of the tube was connected to a 500-mL glass jar to collect falling powder. The horizontal open ends of the PVC tube were closed with stoppers bored to receive a 6.35 mm (1/4”) I.D. tube connector. An APS was used to measure the size distribution of the particles in the falling pipe by recording particle counts by aerodynamic diameter in 51 size channels ranging from 0.5 to 20 µm every 1 sec with a total flow rate of 5 L min⁻¹. The inlet to the APS was attached to one connector with a short non-conductive tube and a high efficiency particulate air (HEPA) filter (PN 12144, Pall Corporation, Port Washington, NY) was placed on the opposing side.

We concluded that an APS was appropriate for this device because, even when nanopowders are applied to the device, large agglomerates that are measurable by the APS will make up the majority of the falling aerosol. Furthermore, the standard measured outcome for dustiness is mass of aerosolized dust relative to mass of bulk powder applied; therefore nano-sized particles that cannot be detected by the APS will have little contribution to the total mass measured. The upper size detection of the APS, however, does not allow for enumeration of all particles that would constitute the inhalable fraction (<100µm) so that the outcome measure of the device is restricted to a determination of respirable dustiness. From the ACGIH definition of the respirable particulate matter fraction,⁽²³⁾ 20 µm represents a

sampling efficiency of only 0.003% and therefore an instrument that measures up to 20 μm captures almost the entire respirable fraction.

Nanoparticle Powders

Ten nanoparticle powders and four other powders were tested. Table 1 gives the median primary particle size and manufacturer of each powder type. Two titanium dioxide (TiO_2) and two aluminum oxide (Al_2O_3) powders with different primary particle sizes were chosen to determine whether the primary size of the same nanopowder affects dustiness. The 21-nm TiO_2 has the trade name Aerioxide[®] P25. Arizona Road Dust (ARD, ISO Standard 12103-1, A2 Fine), Cloisite[®] and Nanofil[®] and reagent-grade TiO_2 were chosen to compare with the dustiness of nanopowders because they represent commonly used powders in a variety of industries. ARD is a standardized dust with well characterized properties that can be considered those of a loosely agglomerated sandy texture. Cloisite[®] is a natural montmorillonate (soft clay) used in plastics and rubber manufacturing. Nanofil[®] is based on natural bentonite clay and also used in plastics manufacturing. Reagent grade TiO_2 was analyzed to compare with the two TiO_2 nanopowders given its larger median particle size (based on microphotography as explained below). Aluminum oxide nanowhiskers (Al_2O_3 whiskers) and single-walled carbon nanotubes (SWCNT) were chosen to represent nanopowders with fibrous particles. The Al_2O_3 whiskers also have the same chemical composition as the other two aluminum oxide (Al_2O_3) nanopowders. Copper was the only pure (99.8%) metal tested in comparison with the metal oxides: iron oxide (Fe_2O_3), silicon dioxide (SiO_2), TiO_2 , and Al_2O_3 . The SiO_2 is a form of fumed silica with the trade name Aerosil[®] 90 that is very “fluffy” and so was chosen as a type of nanopowder that may be easily dispersed when handled. The carbon black tested, with the trade name Printex[®] 90, is not a modern engineered nanopowder but does consist of primary particles in the nanometer range and has been used extensively in industries such as tire manufacturing.

All powder samples were stored in air-tight sealed glass vials. Before using a powder sample in the experimental setup, the vials were opened and placed in an oven (Fisher Isotemp Oven Junior Model, Thermo Fisher Scientific Inc., Pittsburgh, PA) at 120° Celsius for a 24-hour period in order to eliminate moisture in the sample. Our experience with filter samples containing dusts has shown that a temperature slightly above 100°C produces more consistent drying by driving moisture from the interstitial spaces, whereas Method 15051 calls for a drying temperature of 100°C. Although these environmental conditions may vary in actual settings, this method standardizes the powder preparation in order to minimize the influence of moisture content on the dustiness of powders.

Table I provides the mass density and bulk density as well as moisture content for each powder type. Mass density was obtained from sources such as manufacturer's information or material data safety sheets. Bulk density represents the weight per volume of the powder including void spaces. Given the lack of information on all powder types from vendors, a measure of the bulk density was obtained using a modification of an ASTM method.⁽²⁴⁾ Instead of using the prescribed tapping apparatus, a 100 mL graduated cylinder was tamped by hand on a hard surface 5 times before measuring the resulting volume. The cylinder was pre- and post-weighed to determine the mass of the powder which resulted in a measure of bulk, or “tapped”, density by dividing the mass by the volume of the tamped powder. This was also performed on two powders with a reported bulk density, ARD and 21-nm TiO_2 , which resulted in measured values identical to the reported values shown in Table I. Furthermore, the dust moisture content was measured by weighing a sample of each dust type before and after being placed in a 120°C oven for 12 hours.

Test Protocol

Three trials were conducted for each powder type. Each trial used 15 mg of the given powder sample. A piece of aluminum foil was tared and the powder weight measured on a three-place digital balance scale (PE 360 Delta Range, Mettler-Toledo, Inc., Columbus, OH), with an accuracy of ± 1 -mg. The foil was creased and the powder was manually added to the closed ball valve at the top of the drop pipe. All trials were completed within a 12-hour time period to minimize changes in laboratory relative humidity (RH) and temperature. The RH and temperature was measured using a Q-Trak (Model 8551, TSI Inc., St. Paul, MN). The temperature remained constant at $23.9^\circ\text{C} \pm 2^\circ\text{C}$, while the humidity ranged from 45.4 – 47.2% during the 12-hr time period required to complete all trials.

After loading the ball valve with powder an APS sampling run was started. After 10 s, the ball valve was manually turned to release the powder and then immediately closed. The APS recorded count concentrations for another 90 s. Closing the valve prevented a flow of air down through the tube via the APS sample pump so that all sample air had to enter through the HEPA filter opposite the APS inlet tube. Data from the first 9 of the 10 s prior to opening the valve were used as background values. These counts were consistently either 0 or, at most, 1 cm^{-3} in each channel. Preliminary trials indicated that the pulse of measureable aerosol reached a baseline level after 20 s and that the peak occurs 3 to 4 s after the valve was opened.

Calculations—Respirable mass concentrations were calculated from the APS output accumulated for each trial run. The mass of respirable dust produced throughout the entire pulse of measureable particles was determined from the total of the differential count concentrations (referred to as “dW” in the instrument software) in each of the APS size channels. To ensure that the entire pulse was measured, the counts during the 30 s after opening the valve were summed in each size channel. First the summed counts in each size channel, dN_{ae} ($\#/cm^3$), with median aerodynamic diameter, d_{ae} (μm), were transformed to mass concentration, dM_{ae} (mg/m^3), using the following equation: ⁽²⁵⁾

$$dM_{ae} = dN_{ae} \frac{\pi}{6} d_{ae}^3 \quad \text{Eq. 1}$$

This mass concentration, based on a particle with unit density, was then adjusted for the mass density of the powder, ρ_p , to obtain a mass concentration of volume equivalent diameter, dM_v .^(26–27)

$$dM_v = dM_{ae} \left(\frac{\rho_o C_{ae} \chi}{C_{ve}} \right)^{3/2} \frac{1}{(\rho_p)^{1/2}} \quad \text{Eq. 2}$$

with the exception that the middle term in brackets was forced to unity by assuming that the Cunningham correction factor for the aerodynamic diameter, C_{ae} , the Cunningham correction factor for the volume equivalent diameter, C_{ve} , and the aerodynamic shape factor, χ , were equal to 1.0, and that ρ_o is unit density. This assumption is valid under the premise that the majority of particles are spherical in shape ($\chi = 1$), and greater than $1\text{ }\mu\text{m}$ for which C is 1.15 and falls to 1 for larger particles ($> 10\text{ }\mu\text{m}$).⁽²⁶⁾

The mass of all particles per size channel (m_t , mg) was then calculated with Eq. 3:

$$m_t(dM_v)Qt \quad \text{Eq. 3}$$

where Q is the sample flow rate = 0.005 m³/min, t is time = 1/60 min. Then, using the ACGIH definition to determine the respirable fraction for each size channel, η_r , the respirable dustiness of a powder (D , mg/kg) was calculated with Eq. 4:

$$D = \frac{m_t \eta_r}{m_b} \quad \text{Eq. 4}$$

where m_b is the mass of the bolus of powder applied to the LMDT = 15 x 10⁻⁶ kg for all tests performed during this study.

Electron Microscopy Procedures—Scanning electron microscopy (SEM) was utilized to observe the morphology of the aerosol created by the falling powder. To collect representative samples onto an SEM stub, either a thin sheet of mica or filter paper was adhered to the stub which was placed at the bottom of the tube. A small amount (~ 5 mg) of powder was allowed to fall through the tube with the APS sampling pump turned off. SEM photography was performed at The University of Iowa Central Microscopy Research Facility with a Hitachi S-4800 Scanning Electron Microscope (Hitachi High Technologies America, Inc., Pleasanton, CA). The stubs were placed into a chamber and exposed to argon (Emitech Systems K550 Sputter Coater; Quorum Technologies, West Sussex, United Kingdom) in order to eliminate electrical charges on the stub. Transmission electron microscopy (TEM) was also used to view the primary particles within powder agglomerates. These were not sampled from the falling powder but derive from the bulk powder manually applied to the TEM grids.

Statistical Analysis—A one-way analysis of variance (ANOVA) with Tukey's post-hoc analysis of differences between the D value obtained for each powder type was performed. A confidence level of 95% was considered significant. A multi-variable regression analysis was also performed to determine whether D can be predicted given the continuous independent variables mass density, bulk density, void space, and moisture content, and a dichotomous variable to indicate whether or not a powder consisted of granular nanoparticles. Void space is calculated by:⁽²⁸⁾

$$\text{void space} = 1 - \frac{\text{bulk density}}{\text{mass density}} \quad \text{Eq. 5}$$

RESULTS

Concentration pulses created by representative powders are given in Figure 2. The curves in Figure 2 are the average of counts made for each of the 3 trials performed for each powder for the size bin with a median diameter of 2.2 μm. The peak in the pulse occurred within 3 to 4 seconds after the valve was opened for all powder types, and, as shown in Figure 2, the pulse decayed to near 0 counts after 20 seconds. Photomicrographs of particles collected at the base of the vertical tube from representative powders are provided in Figure 3. In general, there was a wide range in particle sizes for all powder types but the majority of particles were > 1 μm. Likewise, at a magnification needed to see the full range of agglomerates present in the falling powder it was not possible to distinguish the individual primary nanoparticles. Those primary particles can be seen in Figure 4 where transmission electron micrographs of agglomerates from some of the smallest particles found from two different TiO₂ powders are shown.

The reproducibility of this method was evaluated by determining the coefficient of variation (CV) for respirable concentrations for each powder type. The average CV for all powders

was 19.2%. The reagent TiO₂ and Cloisite 20A had the highest CV (>33%), and low CV's were obtained when dropping the 10-nm Al₂O₃ and 50-nm Al₂O₃ (<9%).

Table II provides the count (CMAD) and mass median (MMAD) aerodynamic diameters, and the corresponding geometric standard deviation (GSD), averaged for the three trials performed with each dust type. The average size distributions of 3 trials at the peak concentration for four representative powders are shown in Figure 5. The CMAD ranged from 1.46 – 2.40 μm. MMAD values were computed from the CMAD and GSD⁽²⁷⁾ and ranged from 3.48 – 31.11 μm, corresponding to ARD and 10-nm Al₂O₃, respectively. The variation in the CMAD over the time period of a pulse for representative powders is given in Figure 6. The time course shown in Figure 6 for each powder ended when counts shown in Figure 2 fell below 5 cm⁻³ at which point a size distribution could not be accurately determined. In general the CMAD remained relatively stable over the sample time. The aerosols produced by the falling powders did not create an exceedingly wide-range in sizes as evidenced by the relatively low GSD values which ranged from 1.63 – 2.30. As shown in Figure 5, the entire distribution of particle sizes produced in the LMDT occurred within the limits of the APS sizing range for most powder types.

D values for each powder type are reported in Table III and ranged from 3.9 for Cu to 121.4 for SiO₂. Table III also contains a column to indicate a dustiness classification for each dust type. The classification was based on that provided in EN 15051 for the rotating drum. An analysis of the four category names (“very low” to “high”) relative to the dustiness mass fraction limits for each revealed the application of an exponential increase of the form, limit = $k \exp(\ln(5)x)$, where x is a value between 1 and 4 corresponding to the four categories and k has a value of 2. In a similar way, a k value of 0.8 was determined to adequately separate the D values obtained here into 4 classifications with limits of <4, 4 – 20, 20 – 100, and > 100 corresponding to categories of “very low”, “low”, “moderate”, and “high”, respectively.

The ANOVA analysis for respirable dustiness revealed a significant difference between powder types (p<0.001). Results from the Tukey's procedure showed SiO₂ produced significantly higher concentrations than all other dusts after which there were overlapping associations between the remaining dust types (Table III). 5-nm TiO₂ and 21-nm TiO₂ were next highest but less than half of the value for SiO₂. Powders producing low respirable concentrations included Al₂O₃ whiskers and Cu.

The comparison of TiO₂ powders also demonstrated a decline in D with an increase in primary particle size. We were unable to find a manufacturer's report on the reagent TiO₂ but the TEM photos of that dust (Figure 4b) demonstrate primary particles ranging in size between 50–250 nm. Likewise the 10-nm Al₂O₃ is dustier than the 50-nm Al₂O₃.

An analysis of the five factors that may best predict respirable revealed that mass density (ρ_m), log-transformed values of bulk density (ρ_b), and the dichotomous variable to indicate whether the powder had nanosized particles (N) produced significant coefficients with $r^2 = 0.80$. The resulting regression equation for predicting respirable dustiness is:

$$D = 18.97 - 17.723 \ln \rho_b - 6.818 \rho_m + 30.950 N \quad \text{Eq. 6}$$

DISCUSSION

A single-drop, low-mass powder dustiness tester that utilizes 15 mg of powder per test was capable of distinguishing the respirable dustiness of various powder types. The mass of powder applied to each test was sufficient to provide measureable counts in each of the APS size channels without exceeding its count/channel limit (1,000/cm³) (although a

commercially-available diluter is available for the APS). The use of an APS was a departure from the specifications for a single-drop dustiness tester described in DIN 55992-2. However, using a particle counter that sized by aerodynamic diameter permitted calculations to determine the mass of powder collected along with the size segregation needed to estimate a respirable dustiness mass fraction. By contrast, DIN 55992-2 calls for the use of an aerosol photometer which can indicate mass concentration but cannot size segregate. Another difference between this method and the standard is that the APS requires active sampling whereas the standard dictates the use of a passive photometer. Furthermore, unlike other dustiness testing methods, a measure of the inhalable dustiness cannot be obtained with the LMDT method. Given the emphasis on its use for expensive nanopowders, which are primarily inorganic compounds that primarily effect the pulmonary region, a measure of respirable dustiness is the most relevant of the two for nanopowders.

Using the method described here the powder settling down the tube enters a cross-flow volume where particles that can be captured in the sample flow stream to the APS are measured whereas all others fall through to the collecting jar. Therefore, the results obtained in this study are dependent on the APS sample flow rate, the aspiration efficiency of the entry nozzle to the APS, the cross-fitting geometry that will influence particle mixing and air velocity profiles, and the counting efficiency of the APS. Other researchers that used an APS as part of the sample collection of a dustiness apparatus^(21–29) also point out that the counting efficiency of an APS decreases for particles below 1.0 μm based on studies such as the one by Volcken and Peters.⁽³⁰⁾ However, the APS counting efficiency is higher for the dry particles produced during a dustiness test than for droplets. No correction to the counts obtained from the APS were made to compensate for particle count efficiency.

A Reynolds number in the 6.35-mm I.D. air inlet tube of 1113 for the sample flow rate of the APS indicates laminar flow and thus suggests that the inlet flow from the HEPA filter does not produce a turbulent jet to disturb and mix falling particles as they pass through the sampling volume. Particle capture into the exhaust tube to the APS is therefore a function of the terminal settling velocity of the particles relative to the horizontal velocity created in the sampling volume as well as the turning radius provided to deflect particles into the exit tube.

The aerosol size distribution data given in Table II indicates that the distribution of particles produced by this dustiness testing method produced many micrometer-sized particles from nanopowders due to the agglomeration of the primary particles. As particle size decreases, attractive forces such as van der Waals, electrostatic and covalent, increasingly favor the formation of agglomerates.⁽²⁸⁾ This suggests the creation of a bimodal distribution consisting of small agglomerates at the low end, and large unseparated clusters at the high end of the distribution. A bimodal distribution of this sort has been reported by researchers who used both an APS and a scanning mobility particle sizer to measure the size distribution between 10–10,000 nm exiting a rotating drum tester.^(21,29) However, the standard index of dustiness reported in other studies is on a mass-per-mass basis. Therefore, there may be an interest in determining the counts of particles in the nanometer range but their mass will be negligible compared to micrometer-sized particles. Thus an APS, which measures the heavier micrometer-sized particles, is sufficient for determining the dustiness mass fraction.

An APS would not be an adequate measurement device if the dustiness tester reduced a nanopowder to an aerosol with an entire distribution of diameters below 1 μm ; in which case the APS would not adequately detect the many resulting particles that could contribute to a respirable mass. For this to occur, the tester would have to impart enough energy to reduce the bulk powder to nano-sized agglomerates. However, Liden suggests that dustiness tester should not impart enough energy to “divide the primary particles.”⁽⁸⁾ For a settling dust, the most important energy addition would be that from turbulent air flowing around the

powder as it fell. As explained by sources on this subject,^(28,31) an analysis of turbulence is complicated by the large differences in particle sizes and that the falling powder will achieve, each with different settling velocities, a bulk movement with maximum velocity at the center and less in the outer region. However, after applying ten different nanopowders to the device, all produced distributions with median diameters in the micrometer range. Therefore, it may be concluded that the settling bolus of powder in the tester tube does not produce enough energy to break up the powder so that the majority of the particles are less than the lower limit of detection of the APS.

The use of an APS to determine particle mass as developed here was based on the assumption that the particles measured are spheres, and those spheres have a density equivalent to the mass density of the compound comprising the powder. The assumption that the particles are spheres is likely most valid for the nanopowders which tend to form large spherical aggregates as shown in Figure 3, whereas the ARD dust, for example, is composed largely of individual irregularly shaped particles. However, the powders comprised of larger, individual particles will have a density close to the mass density of their parent compound whereas the nano-agglomerates will necessarily have void spaces that reduce their density. Although not tested, it may be assumed that this method will then overestimate the dustiness of nanopowders.

Interestingly, density also affects dustiness in a counter-intuitive way. Given counts in bins separated by aerodynamic diameter, to determine the mass of those counts density is used to adjust the size of the particles to their true diameter and then their volume and, ultimately, mass is calculated. High density particles result in smaller physical diameters to have the same settling velocity, which significantly reduces a particle's volume and mass by the cube of diameter. Therefore, for the same number of counts based on aerodynamic diameter made by the APS, higher density particles will result in lower mass and therefore lower dustiness than particles with low density.

In general, our results demonstrated that powders consisting of granular nanoparticles are more dusty than powders with fibrous nanoparticles or powders containing granular particles that are greater than 100 nm. Smaller primary particles are expected to develop smaller agglomerates which will settle more slowly and therefore are more easily captured in the sample stream of the APS. When using a rotating drum, Plinke et al. found a strong positive correlation between particle diameter and dustiness.⁽²⁰⁾ Fibrous nanoparticles, however, are known to develop tightly bound "bird nests" which result, for example, in the difficulty researchers have experienced when trying to generate a carbon nanotube aerosol from the bulk powder.^(32,33) Conversely, the amorphous SiO₂ nanopowder tested visually exhibited a morphology that was light and "fluffy" that readily de-aggregated as it fell through the tube contributing to its exceptionally large dustiness mass fraction.

The majority of other studies conducted to obtain a powder dustiness mass fraction (D) used a rotating drum device.^(18,21,22,29) For example, Tsai et al. obtained a respirable D of 15 mg/kg for the same 21-nm TiO₂ used in this study, which compares to a 45.3 mg/kg using the LMDT.⁽²⁹⁾ Likewise, the EN 15051 dustiness method provides a respirable D of 140 mg/kg for bentonite when using the rotating drum and 170 mg/kg when using the continuous drop method, which can be compared to the Nanofil® 5 respirable D value of 29 mg/kg.⁽¹⁷⁾ Despite differences in the D value obtained, a "moderate" risk category was applied to this powder type via both EN 15051 methods and this LMDT method. Future work will involve a comparison of results obtained with the LMDT with those given in Annex D of EN 15051 for a suite of seven powder types. Bach and Schmidt describe results from a comparison of two alternative dustiness testers that followed the guidelines provided in Annex D.⁽¹⁸⁾ They found it difficult to derive the same classifications as those given in EN 15051 for all

powder types when using the alternative methods but noted that there was a higher equivalency for the respirable particle fraction than for the inhalable fraction. Pensis et al. also compared the rotating drum with the continuous drop tester and found that the respirable mass fractions were comparable, but the continuous-drop tester overestimated the inhalable mass fraction 3 to 17 times higher compared to the rotating drum depending on powder type.⁽²²⁾

CONCLUSION

A low mass dustiness tester (LMDT) designed to report the respirable dustiness from milligram quantities of sample powder was tested with a variety of powder. The LMDT incorporated an APS that permitted a calculation of the respirable dustiness mass fraction from counts in particle size channels delineated by aerodynamic diameter. When applied to a variety of powder types, those consisting of primary particles that were granular and with diameters in the nanoparticle range demonstrated the highest dustiness. The respirable dustiness of SiO₂, a light fluffy powder, was significantly higher than all others. However, many nanopowders were not significantly more dusty than powders containing larger primary particles. A multivariable regression analysis was developed that can be used to estimate the respirable dustiness mass fraction of these powders given the powder's bulk and mass densities and whether it contains nano-sized, granular primary particles. Furthermore, a classification scheme similar to that provided in a standard method for dustiness was developed. The regression model and classification scheme may be useful for efforts to incorporate dustiness as a factor in risk assessment models for the powder and nanopowder industries.

Acknowledgments

This study was funded by NIOSH R01 OH008806-01 in collaboration with the EPA (2005-STAR-B1), and supported by NIEHS P30 ES05605-11.

References

1. Maynard AD. Nanotechnology: the next big thing, or much ado about nothing? *Ann Occup Hyg.* 2006; 51:1–12. [PubMed: 17041243]
2. Mark, D. Nanomaterials: a risk to health at work? Report of presentations at plenary and workshop sessions and summary of conclusions. First International Symposium On Occupational Health Implications, sponsored by British Health and Safety Executive and the United States National Institute for Occupational Safety and Health; Palace Hotel, Buxton, Derbyshire, U.K. October 12–14, 2004; [Online] Available at http://www.hsl.gov.uk/media/1646/nanosymrep_final.pdf (as of September 13, 2011)
3. Maynard AD, Aitken RJ. Assessing exposure to airborne nanomaterials: current abilities and future requirements. *Nanotoxicology.* 2007; 1(1):26–41.
4. Mark, D. The use of reliable measurements of dustiness of chemicals in selecting the most appropriate dust control technology. IOHA 6th International Scientific Conference; Pilanesberg National Park, North West Province, South Africa. September 2005; 2005. p. 1-5.
5. Hamelmann F, Schmidt E. Methods for characterizing the dustiness estimation of powders. *Chem Eng Technol.* 2004; 27(8):844–847.
6. Brouwer DH I, Links H, De Vreede SAF, Christopher Y. Size selective dustiness and exposure: simulated workplace comparisons. *Ann Occup Hyg.* 2006; 50(5):445–452. [PubMed: 16524926]
7. Hamelmann F, Schmidt E. Methods of estimating the dustiness of industrial powders: a review. *KONA.* 2003; 21:7–17.
8. Lid n G. Dustiness testing of materials handled at workplaces. *Ann Occup Hyg.* 2006; 50(5):437–439. [PubMed: 16849593]

9. Heitbrink WA, Todd WF, Cooper TC, O'Brien DM. The application of dustiness tests to the prediction of worker dust exposure. *Am Ind Hyg Assoc J.* 1990; 51(4):217–223. [PubMed: 2327332]
10. Shulte P, Geraci C, Zumwalde R, Hoover M, Kuempel E. Occupational risk management of engineered nanoparticles. *J Occup Environ Hyg.* 2008; 5:239–249. [PubMed: 18260001]
11. Schneider T, Brouwer DH, Koponen IK, et al. Conceptual model for assessment of inhalation exposure to manufactured nanoparticles. *J Expo Sci Environ Epidemiol.* Mar.2011 Advance online publication. 10.1038/jes.2011.4, 2
12. Breum NO, Schneider T, Jorgenson O, et al. Cellulosic building insulation versus mineral wool, fiberglass or perlite: installer's exposure by inhalation of fibers, dust, endotoxin and fire-retardant additives. *Ann Occup Hyg.* 2003; 47:653–69. [PubMed: 14602673]
13. Class P, Deghillage P, Brown RC. Dustiness of different high-temperature insulation wools and refractory ceramic fibres. *Ann Occup Hyg.* 2001; 45:381–384. [PubMed: 11418088]
14. Pujara, CP.; Kildsig, DO. Effect of individual particle characteristics on airborne emissions. In: Wood, JP., editor. *Containment in the Pharmaceutical industry. Drugs and Pharmaceutical Sciences.* Vol. 108. Basel, Switzerland: Marcel Dekker AG; 2001. p. 29-54.
15. Boundy M, Leith D, Polton T. Method to evaluate the dustiness of pharmaceutical powders. *Ann Occ Hyg.* 2006; 50:453–458.
16. DIN 55992-2 (1996, 1999). Determination of a parameter for the dust formation of pigments and extenders - Part 2: drop method. Deutsches Institut Fur Normung E.V. (German National Standard)
17. EN 15051. Workplace atmospheres— Measurement of the dustiness of bulk materials - Requirements and reference test methods. Brussels, Belgium: European Committee for Standardization (CEN); 2006.
18. Bach S, Schmidt E. Determining the dustiness of powders – a comparison of three measuring devices. *Ann Occup Hyg.* 2008; 52:717–725. [PubMed: 18927102]
19. Heitbrink WA. Factors affecting the Heubach and MRI dustiness tests. *Am Ind Hyg Assoc J.* 1990; 51(4):210–216. [PubMed: 2327331]
20. Plinke M, Maus R, Leith D. Experimental examination of factors that affect dust generation by using Heubach and MRI testers. *Am Ind Hyg Assoc J.* 1992; 53:325–330. [PubMed: 1609743]
21. Schneider T, Jensen KA. Combined single-drop and rotating drum dustiness test of fine to nanosize powders using a small drum. *Ann Occup Hyg.* 2008; 52(1):23–34. [PubMed: 18056087]
22. Pensis I, Mareels J, Dahmann D, Mark D. Comparative evaluation of the dustiness of industrial minerals according to European Standard EN 15051, 2006. *Ann Occup Hyg.* 2010; 52(2):204–216. [PubMed: 19955327]
23. American Conference for Governmental Industrial Hygienists. TLVs® and BEIs® Based on the Documentation of the Threshold Limit Values for Chemical Substances and Physical Agents & Biological Exposure Indices. ACGIH®; Cincinnati, OH: 2010.
24. ASTM B 527-06. Standard Test Method for Determination of Tap Density of Metallic Powders and Compounds. ASTM International; West Conshohocken, PA: 2006.
25. Estimation of Mass with the Model 3321 APS Spectrometer. TSI Inc; 2009. Application Note APS-001
26. Baron, PE.; Willeke, K. *Aerosol Fundamentals.* In: Baron, PA.; Willeke, K., editors. *Aerosol Measurement: Principles, Techniques, and Applications.* 2. New York: Wiley-Interscience, Inc; 2001.
27. Hinds, WC. *Aerosol Technology: Properties, Behavior, and Measurement of Airborne Particles.* 2. New York: Wiley-Interscience, Inc; 1999. p. 98
28. Fayed, ME.; Otten, L. *Handbook of Powder Science and Technology.* New York: Van Nostrand Reinhold Co; 1984. p. 231-236.p. 612-614.
29. Tsai CJ, Wu CH, Leu ML, et al. Dustiness test of nanopowders using a standard rotating drum with a modified sampling train. *J Nanopart Res.* 2009; 11:121–131.
30. Volckens J, Peters TM. Counting and particle transmission efficiency of the aerodynamic particle sizer. *J Aerosol Sci.* 2005; 36:1400–8.

31. Ansart R, de Ryck A, Dodds JA. Dust emission in powder handling: free falling particle plume characterization. *Chem Eng J*. 2009; 152:415–420.
32. Maynard AD, Baron PA, Foley M, Shvedova AA, Kisin ER, Castranova V. Exposure to carbon nanotube material: aerosol release during the handling of unrefined singlewalled carbon nanotube material. *J Toxicol Environ Health A*. 2004; 67:87–107. [PubMed: 14668113]
33. Schmoll L, Elzey S, Grassian V, O'Shaughnessy PT. Nanoparticle Aerosol Generation Methods from Bulk Powders for Inhalation Exposure Studies. *Nanotoxicology*. (Epub ahead of print July 22, 2009. 10.1080/17435390903121931
34. Jensen KA I, Koponen K, Clausen PA, Schneider T. Dustiness behavior of loose and compacted bentonite and organoclay powders: what is the difference in exposure risk? *J Nanopart Res*. 2009; 11:133–146.

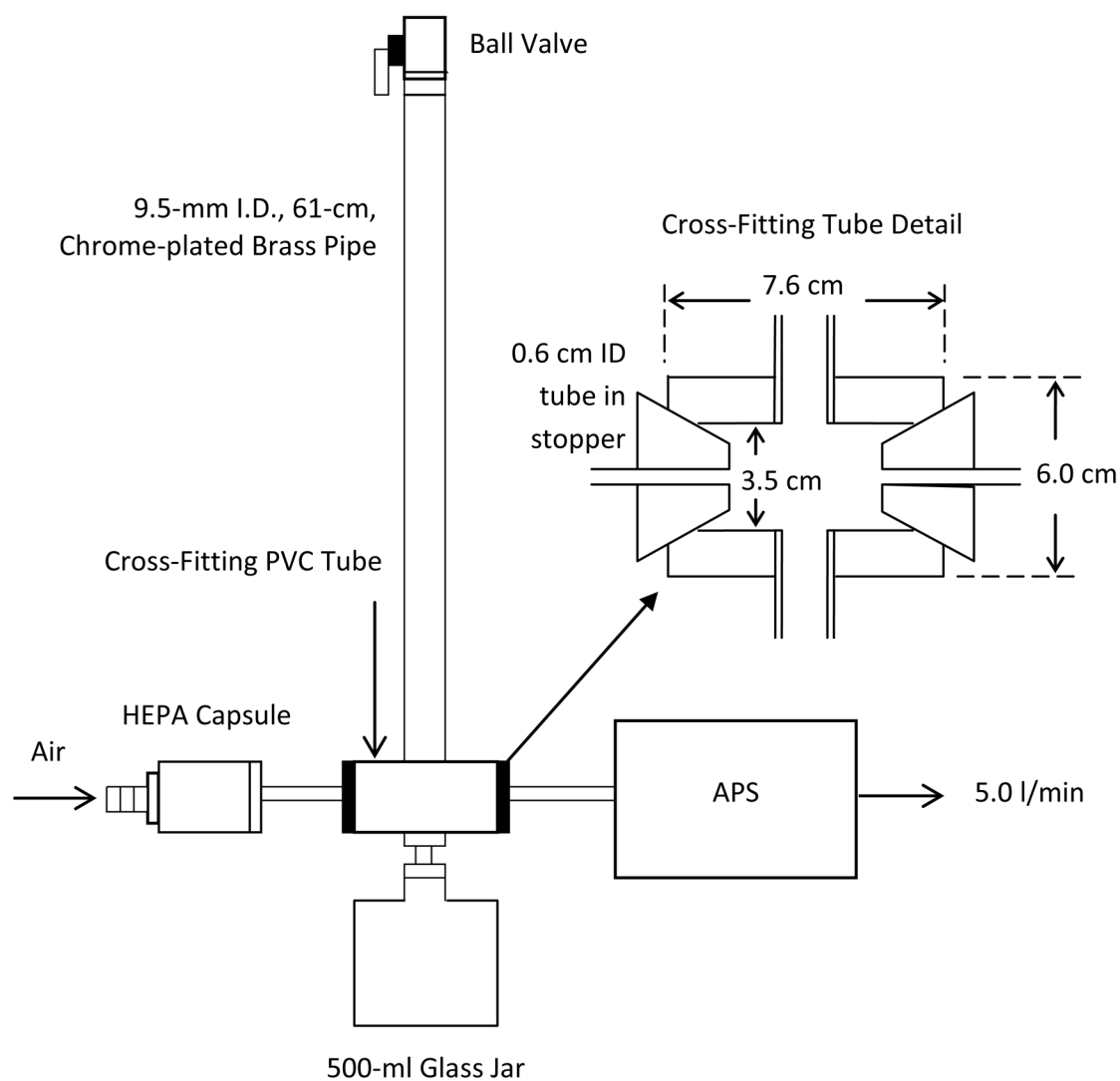


FIGURE 1.
Experimental setup.

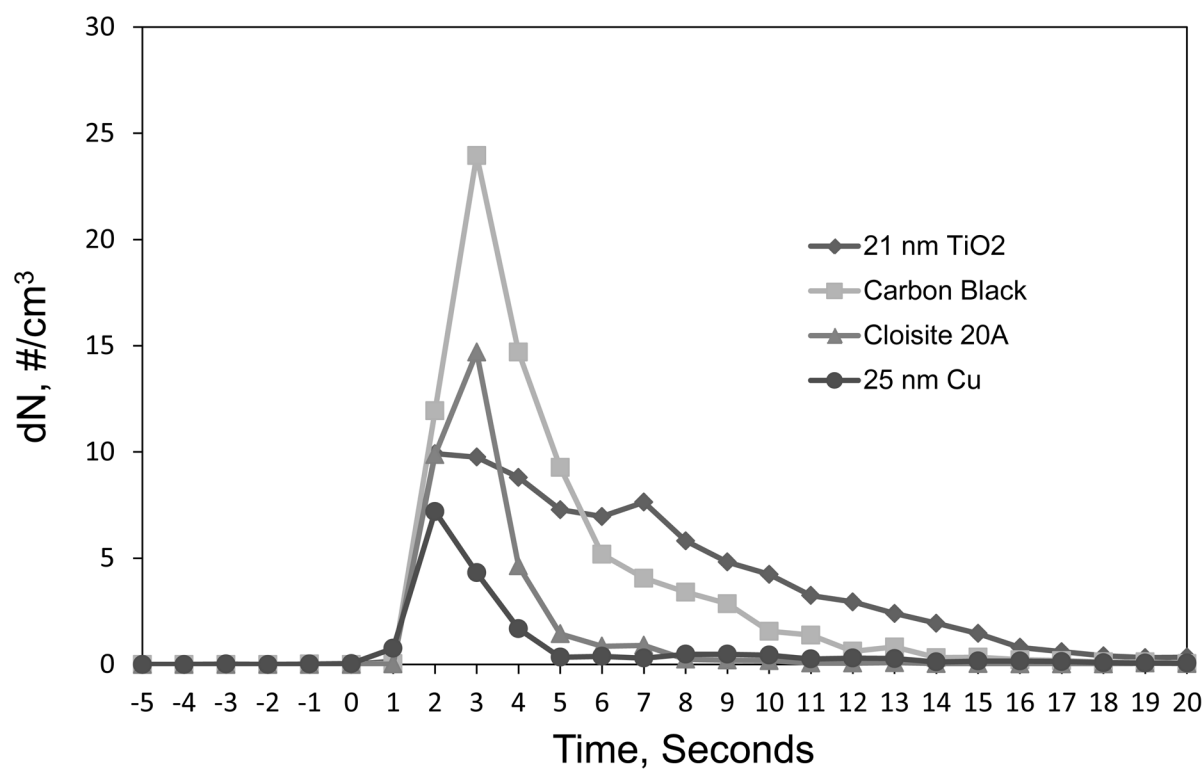


FIGURE 2.
Concentration pulses for four representative powders recorded in the size bin with median diameter of 2.2 μm .

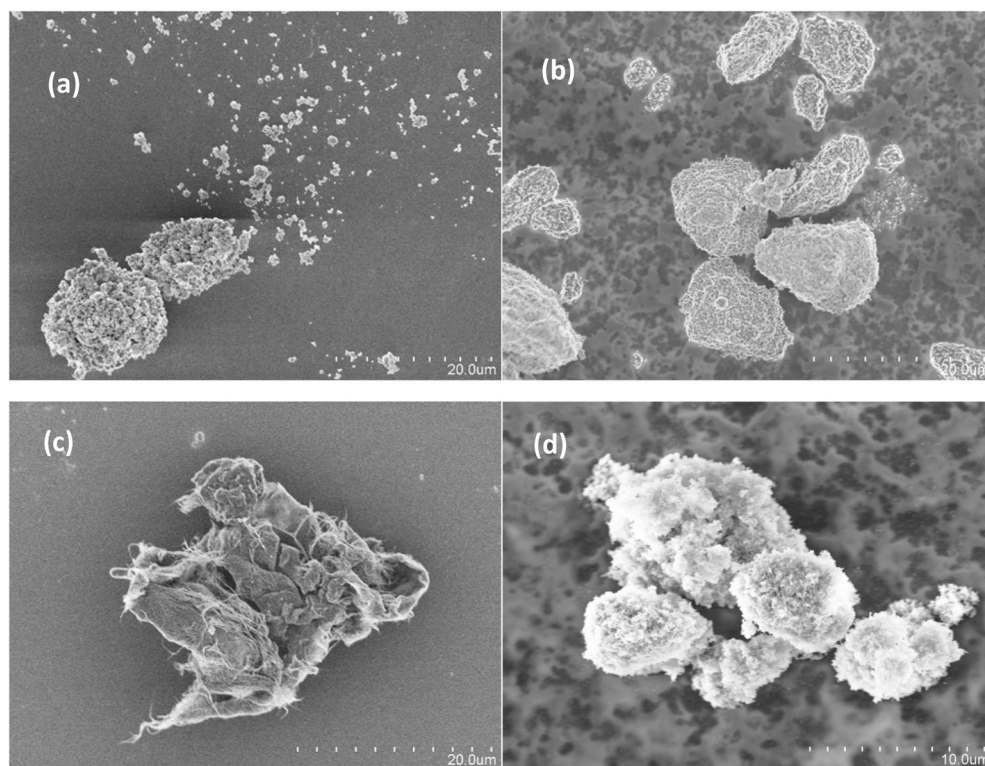


FIGURE 3.

Photomicrographs of particles resulting from the following powders: (a) 5-nm TiO_2 , (b) Fe_2O_3 , (c) single-wall carbon nanotubes, and (d) SiO_2 .

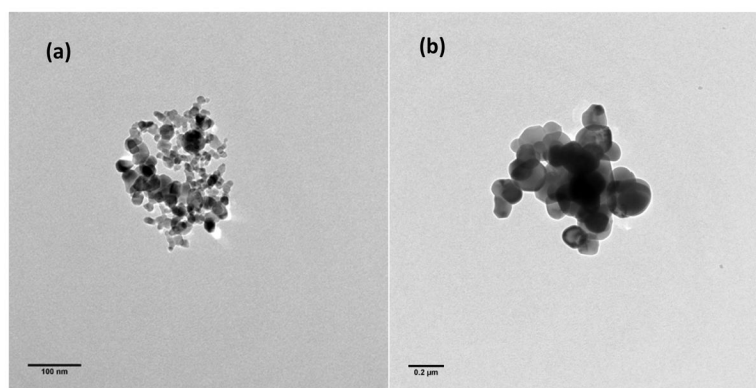


FIGURE 4. Transmission electron micrographs of (a) 21-nm TiO₂ and (b) reagent-grade TiO₂.

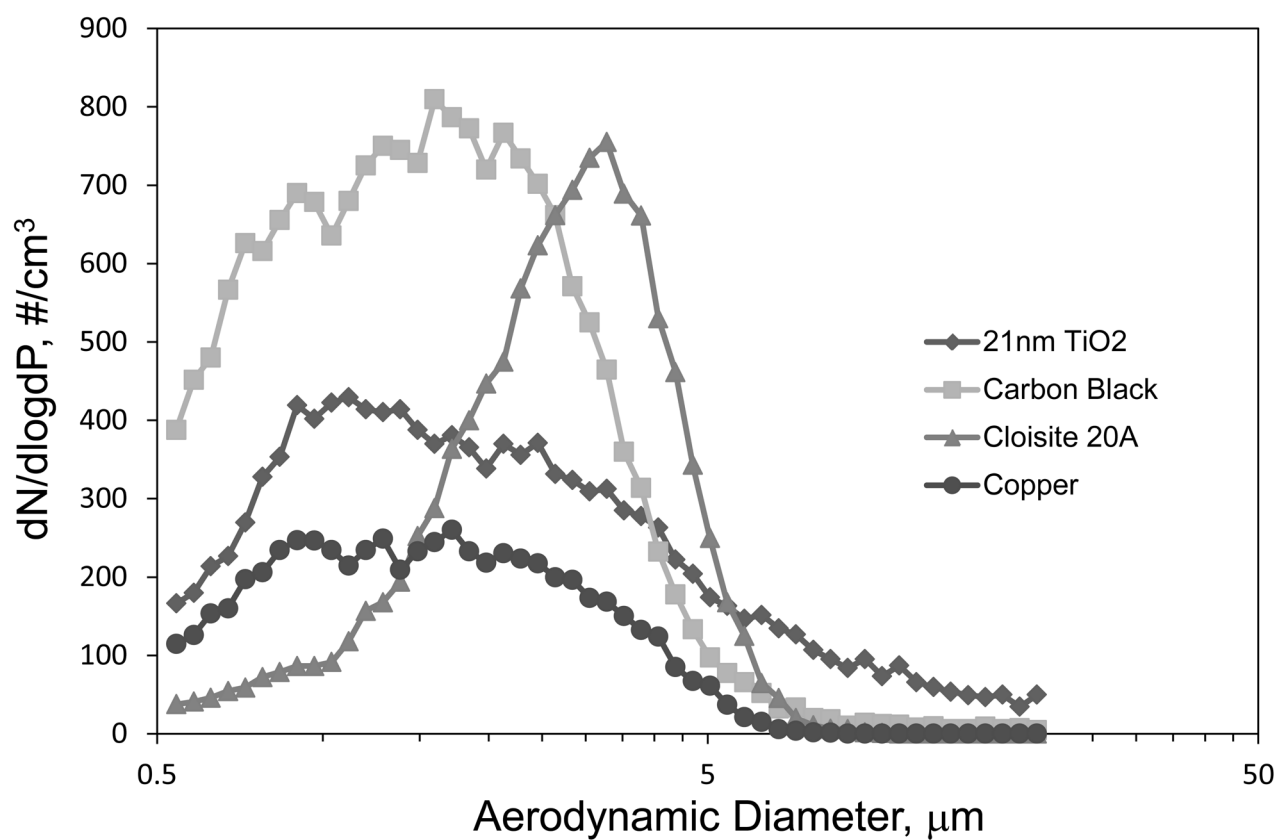


FIGURE 5. Size distributions at the peak concentration for four representative powders.

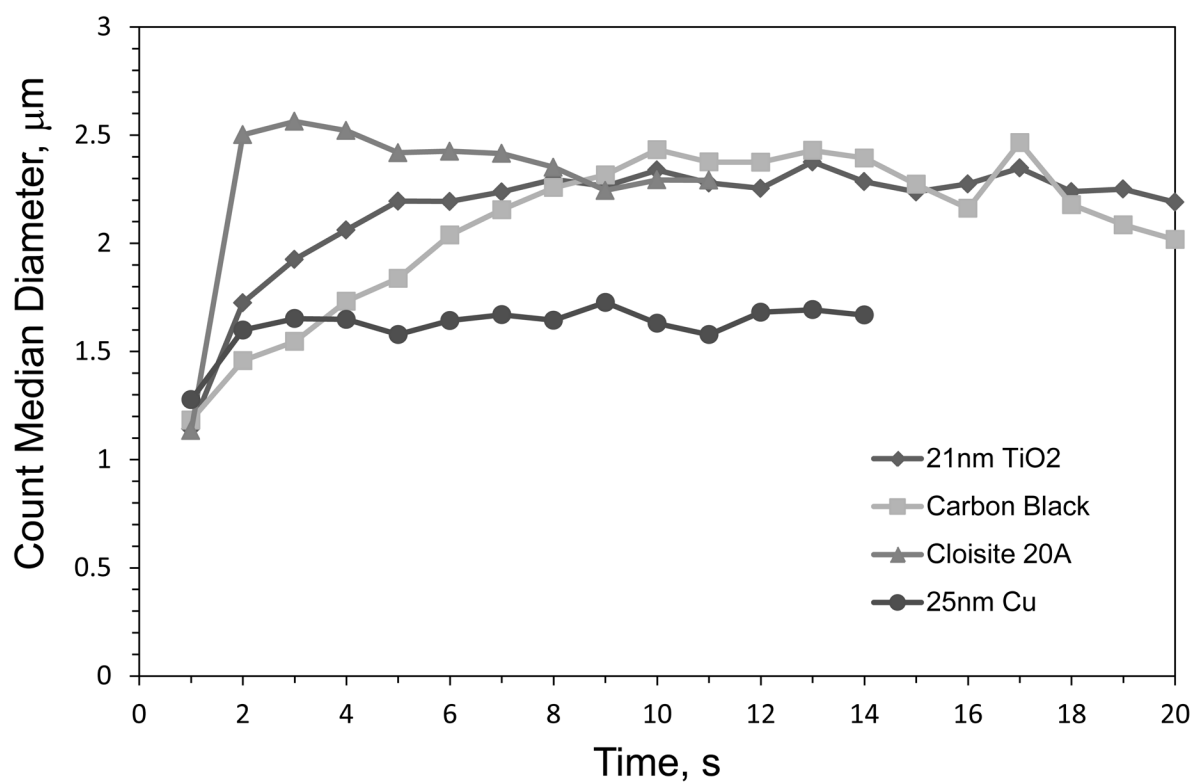


FIGURE 6.
Count median diameter obtained during a pulse for four representative powders.

TABLE I

Properties of Tested Powders

Powder	Median Size, nm	Manufacturer	Mass Density, g/cc	Bulk Density, g/cc	Moisture Content, %
Nanopowders					
Al ₂ O ₃ whiskers	2–4 x 2800	SA ⁴	3.9	0.63 ¹⁰	0.11
Al ₂ O ₃	10	NAM ⁵	3.9	0.24 ¹⁰	0.05
Al ₂ O ₃	50	SA	3.9	1.28	0.07
Carbon Black	14	EDC ⁶	2.0	0.56	0.07
Cu	25	NAM	8.9	0.25	0.01
Fe ₂ O ₃	35	NAM	5.2	1.20 ¹⁰	0.70
SiO ₂	20	EDC	2.2	0.03 ¹⁰	0.20
SWCNT ¹	1–2 x 15,000	NAM	1.4	0.14	0.40
TiO ₂	5	NAM	4.3	0.26 ¹⁰	1.08
TiO ₂	21	EDC	4.3	0.12 ¹⁰	0.19
Other Powders					
ARD ²	9100	PT ⁷	2.7	0.90 ¹⁰	0.26
Cloisite® 20A	6000	SCP ⁸	1.8	0.22	0.23
Nanofil® 5	10,000	SCP	1.6	0.22	0.32
TiO ₂ (Reagent)	NR ³	SL ⁹	4.3	0.77	0.06

¹ Single walled carbon nanotubes

² Arizona Road Dust, ISO Standard 12103-1 A2 Fine

³ Not Reported. TEM photomicrographs reveal particles between 50 – 250 nm

⁴ Sigma-Aldrich, St. Louis, MO

⁵ Nanostructured & Amorphous Materials, Inc., Houston, TX

⁶ Evonik Degussa Corp., Parsippany, NJ

⁷ Powder Technology, Inc. Burnsville, MN

⁸ Southern Clay Products, Inc., Gonzales, TX

⁹ Science Lab.com, Inc. Houston TX

¹⁰ Measured value; all other bulk densities are reported from various sources

TABLE II

Falling Powder Count and Mass Median Diameter and Geometric Standard Deviation.

Powder	Median Size, nm	Count Median Diameter, μm	Mass Median Diameter, μm	Geometric Standard Deviation, μm
Nanopowders				
Al ₂ O ₃ whiskers	2–4 x 2800	1.72	6.23	1.92
Al ₂ O ₃	10	2.40	31.11	2.52
Al ₂ O ₃	50	1.86	7.10	1.92
Carbon Black	14	1.55	4.63	1.83
Cu	25	1.60	4.51	1.80
Fe ₂ O ₃	35	1.86	8.72	2.05
SiO ₂	20	1.78	4.68	1.76
SWCNT ¹	1–2 x 15,000	1.59	6.91	2.01
TiO ₂	5	2.08	16.82	2.30
TiO ₂	21	2.07	15.55	2.26
Other Powders				
ARD ²	9100	1.46	3.48	1.71
Cloisite® 20A	6000	2.58	5.29	1.63
Nanofil® 5	10,000	1.69	3.69	1.67
TiO ₂ (Reagent)	NR ³	1.59	4.51	1.93

TABLE III

Respirable Dustiness Mass Fractions with Standard Deviation Ordered by Dustiness.

Powder	Median Size, nm	Respirable Dustiness, mg/kg	Tukey's Analysis^I	Dustiness Classification
SiO ₂	20	121.4 (14.6)	A	High
TiO ₂	5	60.4 (5.7)	B	Moderate
TiO ₂	21	45.3 (8.5)	B C	Moderate
Carbon Black	14	42.9 (6.0)	B C	Moderate
Al ₂ O ₃	10	40.4 (0.7)	B C D	Moderate
Nanofil® 5	10,000	29.0 (4.1)	C D E	Moderate
Cloisite® 20A	6000	28.2 (9.4)	C D E F	Moderate
SWCNT ^I	1–2 x 15,000	21.1 (2.6)	D E F G	Moderate
TiO ₂ (Reagent)	NR ³	18.2 (13.1)	E F G	Low
Al ₂ O ₃	50	16.5 (1.5)	E F G	Low
Fe ₂ O ₃	35	8.1 (0.8)	F G	Low
ARD ²	9100	6.8 (0.8)	G	Low
Al ₂ O ₃ whiskers	2–4 x 2800	6.7 (1.2)	G	Low
Cu	25	3.9 (1.3)	G	Very Low

^I Equivalent letters indicates not significantly different for $\alpha = 0.05$.